OPTIMIZED SLITTING PARAMETERS FOR THE SHEAR SLITTING OF PAPER

by

E. Wolf and E. G. Welp
Ruhr-University Bochum
GERMANY

ABSTRACT

Due to the demand for an increasing quality of cutted or slitted products and the requirement of rising productivity in the slitting process, the optimization of mechanical slitting is gaining in importance for the converting industry.

In this paper the shear slitting process is analysed theoretically on the basis of a nonlinear orthotropic material law. In a basic investigation the states of stress and strain in the compression phase of the slitting process are discussed. The following application oriented calculations investigate the influence of individual parameters and lead to the suggestion of an optimal cutting tool geometry depending on the material to be cut.

NOMENCLATURE

E_1^{ini+}	tensile initial Young's modulus in MD
S_1^{+}	boundary tensile stress in MD
E_1^{ini-}	compressive initial Young's modulus in MD
S_1^{-}	boundary compressive stress in MD
E_2^{ini}	initial Young's modulus in ZD
ε_2^{max-}	boundary compressive strain in ZD
G_{12}^{ini}	initialer shear modulus in the MD-ZD - plane
S_{12}	boundary shear stress in the MD-ZD - plane
A_{S12}	shear hardening parameter
B_{S12}	shear hardening parameter
μ_{12}	Poisson's ratio in the MD-ZD - plane

INTRODUCTION

Due to the demand for an increasing quality of cutted or slitted products and the requirement of rising productivity in the cutting process, the optimization of mechanical slitting is gaining in importance for the converting industry of thin, plane materials. Because

of the high costs per slitting section and still not met requirements arising from practical use, alternative slitting techniques such as water jet- or laser beam cutting haven't been established yet in paper converting.

The **mechanical cutting** is the most common technique used for separating in paper converting. Stroppel [1] defines it "as a mechanical separating process of a material by means of a cutting tool, whose wedge-shaped blade geometry separates the formation of the material due to high particular normal and shear forces along the cutting edge by exceeding its plastic deformability". The shear slitting process, as a specific kind of mechanical cutting and as the emphasis of this investigation is described as the fragmentation of a material by the blades of two workpieces, moving relative to each other, whereby the material failure occurs due to the material gliding in the slitting zone [2].

Typical converted or finished materials are paper (as generic term for paper, board or corrugated board), films or metal foils. The initial shape of these materials is a wide web, which is longitudinally slitted continuously into narrower rolls or cross cutted discontinuously into sheets.

Preceeding analyses of the shear slitting process [3] of paper and board showed, that the separation process takes place in three phases: the compression-, the slitting- and the tearing phase. The transition between these individual phases depends on the specific failure parameters, which are the shear-yield- and the shear-break-boundary. Up to now this three-phase-hypothesis based on the failure properties of paper hasn't been explicitly proofed. Analysing the state of research has shown, that there are still no systematical and complete investigations to optimize the slitting results by finding the best combination of slitted material, slitting procedure and cutting tool. Furthermore there is no material law available for paper, that describes the real anisotropic load-deformation behavior from the initial range of deformation up to failure and thereby allows an investigation of the slitting process.

Using a simplified material law for paper the kinetics of the slitting zone and the failure hypothesis for the shear slitting of paper were examined in numeric calculations with the finite-elemet-method (FEM) [3]. Because of the used simplified material law only a qualitative separation of the individual slitting phases by means of the load direction and load type dependent material boundaries of paper was possible.

Starting from this initial situation this paper investigates the shear slitting of paper on the basis of different material laws. The aim is to describe the transition between the compression- and the slitting-phase as the initiating process of slitting in a more realistic way and with that, to be able to suggest an optimal cutting tool geometry in dependence of the slitted material.

THE LOAD-DEFORMATION BEHAVIOR OF PAPER

The material paper can be considered in its geometrical structure as a three-dimensional network of fibers, where the cell and/or wood pulp fibers as well as the additives are aligned irregularly. This structural inconsistency of paper causes a strong inhomogenity, significantly influencing the load-deformation behavior from the initial range of loads up to the failure range.

Due to the load conditions occuring in individual production, finishing and converting processes there are three main directions of material symmetry in a paper web, the machine direction (MD), the cross direction (CD) and the thickness direction (ZD). For calculation purposes this means, that the anisotropic material paper can be modelled as an orthotropic material [3], [4] and [5].

In case paper is loaded normally in one of these main directions or with shear in one of the three main planes, it exhibits a nonlinear load-deformation behavior, that is dependent on the load direction and load type (see fig. 1). Independent of the normal load direction there is always a degressive dependency for tensile loads and a progressive dependency for compressive loads.

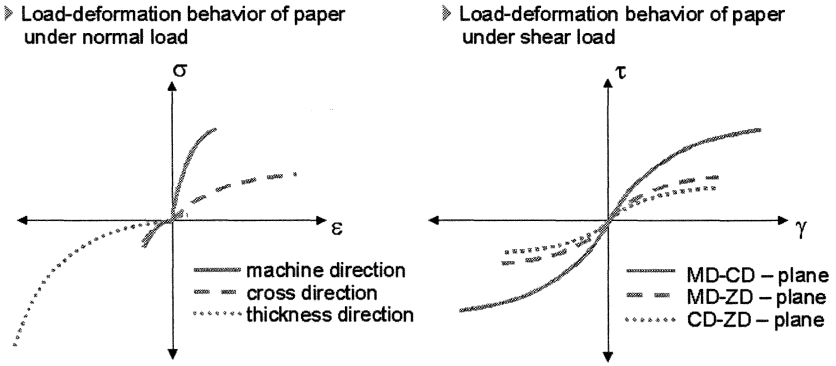

Fig. 1: Load-deformation behavior of paper subjected to normal loading

The stress-strain-curves for normal loading show the different stiffness and failure properties emphazising the dependency of the material behavior on the load direction. The state of material failure under tensile load is characterized by a tensile boundary stress for all directions. Contrary to this, it is not possible to determine an explicit state of failure or a boundary stress for any of the three main directions under compressive loads. Therefore the state of highest compression is not characterized by a boundary stress but a boundary strain. In MD and CD the compressive failure is characterized by folding. Because of the porous material structure the compressive stress-strain behavior in thickness direction shows, compared to the other directions, the largest deformation range, whereas for both tensile and compressive loads the highest stiffness is exhibited by the machine direction.

Under shear loading, which represents the most important state of loading for the slitting process, paper exhibits a nonlinear, degressive load direction dependent stress-strain behavior comparable to the tensile stress-strain behavior. The following figure contains qualitative shear stress-strain curves as determined by [5]. Again the load direction dependency is reflected in the stiffness and failure properties of the material (fig. 1).

The described elementary states of load form the basis for calculating the load-deformation behavior with constitutive laws. The states of load occuring in converting processeses, e.g. in slitting, are determined by a combination of these elementary states. To reach a basic understanding of the shear slitting process it is necessary to investigate the combined load-deformation of paper.

Up to now the material behavior of paper under combined loads was mainly investigated for biaxial tensile loading in MD and CD [6]- [8]. Accordingly, the uniaxial tensile load-deformation behavior in one of the main directions is strongly influenced by a tensile load in the second direction. The material failure under biaxial tensile stress shows a squared failure surface in the stress space and can be described with the Tsai-Wu failure hypothesis [7].

Investigations regarding load-deformation behavior of paper subjected to combined compressive ZD loading and shear loading in the MD-ZD- or CD-ZD-plane, were presented by Stenberg [5] and Waterhouse [9]. Both works describe the shear behavior to be greatly

dependent on the applied compressive load. With increasing compressive loads the shear behavior gets stiffer and the failure boundaries rise (fig. 3). Stenberg presented a yield and failure surface for shear loads in the MD-ZD-plane and normal loads in ZD (fig. 3).

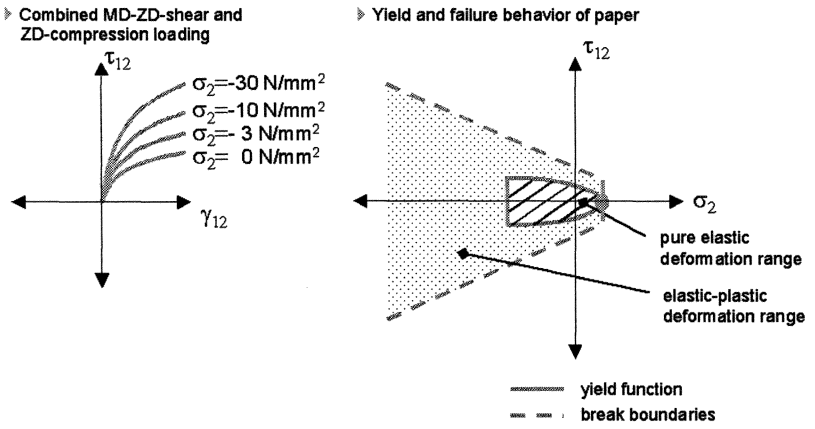

Fig. 3: Load-deformation of paper under combined load in the MD-ZD - plane

Investigations to the load-deformation behavior of combined MD tension and MD-ZD or CD-ZD shear as well as combined MD or CD tension and ZD compression are not known up to now.

Constitutive laws to describe the presented uni- and multiaxial load-deformation behavior for all three main directions of paper from the initial range of loads up to the range of failure are also not known. Merely the material laws by Paetow [4] and Xia [10], that model the two-dimensional "in-plane" load-deformation behavior of paper and the uniaxial material laws presented by van Haag [11] and Pfeiffer [12] for the description of ZD compression are to be mentioned in this context. The only constitutive law that includes the combination of shear loads in the MD-ZD- or CD-ZD-plane and ZD compression as well as the description of the elastic and plastic properties of paper has been developed by Stenberg [5].

MODELING OF THE LOAD-DEFORMATION BEHAVIOR OF PAPER

For the numerical calculations of the shear slitting process a material behavior idealisation in form of a nonlinear elastic orthotropic is used. The coordinates as well as the stress and strain definition presented in the following figure have been used for the material law.

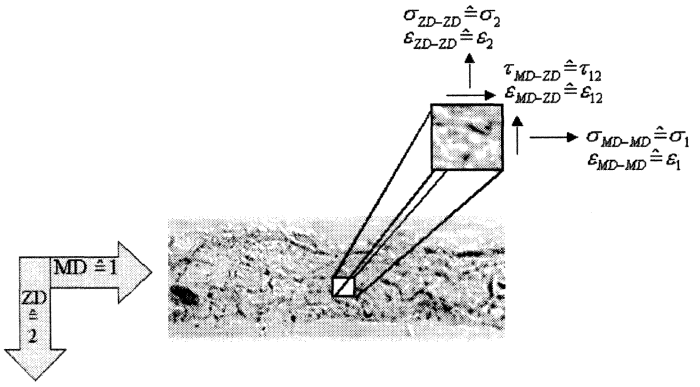

Fig. 4: Coordinates and definition of the stress and strain variables

Generally the orthotropic material behavior is used to describe the load-deformation behavior of materials with orientation dependent properties. The theoretical and experimental investigations of Paetow [4] and Stenberg [5] have shown, that the material behavior of paper can be assumed to be orthotropic in all directions. For the description of orthotropic load-deformation behavior in two dimensions the following material law can be used:

$$\begin{pmatrix} \sigma_1 \\ \sigma_2 \\ \tau_{12} \end{pmatrix} = \begin{pmatrix} \frac{E_1}{1-\nu_{12}\nu_{21}} & \frac{\nu_{12}E_2}{1-\nu_{12}\nu_{21}} & 0 \\ \frac{\nu_{12}E_2}{1-\nu_{12}\nu_{21}} & \frac{E_2}{1-\nu_{12}\nu_{21}} & 0 \\ 0 & 0 & G_{12} \end{pmatrix} \cdot \begin{pmatrix} \varepsilon_1 \\ \varepsilon_2 \\ \gamma_{12} \end{pmatrix} \qquad (1)$$

Considering that paper exhibits a strong nonlinear behavior in all main directions, formula (1) has to be extended. In the compliance law by Paetow (2) the nonlinearity is described with use of a nonlinear, orientation dependent term. This term was extended for all kind of load types and paper main directions and coupled with the linear stiffness matrix of formula (1) for orthotropic materials. Thus the normal and shear stresses can be calculated with the two-dimensional, load direction and load type dependent, nonlinear material law for paper (2).

$$\sigma_1 = \frac{\varepsilon_1}{1-\nu_{12}\cdot\nu_{21}}\cdot\left\{\begin{array}{l} E_1^{ini+}\cdot\left(\dfrac{1}{1+\dfrac{E_1^{ini+}}{S_1^{+}}\varepsilon_1}\right) \text{ for tensile load in MD} \\ E_1^{ini-}\cdot\left(\dfrac{1}{1+\dfrac{E_1^{ini-}}{S_1^{-}}\varepsilon_1}\right) \text{ for compressive load in MD} \end{array}\right\} + \frac{\nu_{12}\cdot E_2^{ini}}{1-\nu_{12}\cdot\nu_{21}}\varepsilon_2$$

$$\sigma_2 = \frac{\nu_{12}\cdot E_2^{ini}}{1-\nu_{12}\cdot\nu_{21}}\cdot\varepsilon_1 + \left(\frac{1}{1-\dfrac{\varepsilon_2}{\varepsilon_2^{max}}}\right)\cdot\frac{E_2^{ini}}{1-\nu_{12}\cdot\nu_{21}}\cdot\varepsilon_2 \qquad (2)$$

$$\tau_{12} = \pm\frac{1}{\dfrac{G^{ini}}{1+\dfrac{12}{S_{12}}\cdot|\gamma_{12}|}}G_{12}\cdot|\gamma_{12}|$$

$$with \left\{\begin{array}{l} + \text{ for } \gamma_{12}\geq 0 \\ - \text{ for } \gamma_{12}<0 \end{array}\right\} \quad and \quad \left\{S_{12} = \begin{array}{ll} A_{S_{12}} + B_{S_{12}}\cdot|\sigma_2| & \text{for compressive load in ZD} \\ A_{S_{12}} & \text{for tensile load in ZD} \end{array}\right\}$$

The advantage of formulating the material behavior in this way lies in the description of each nonlinearity by a single nonlinear term and the possibility to calculate MD-ZD- shear stresses in dependence of the ZD stresses. With this the material hardening under combined load is considered in an easy mathematical way. For the application of this material law all material constants have to be determined by experimental measurements. Tab. 1 presents the values acquired for the paperboard analyzed in this investigation:

Parameter	Description	Value	Experimental setup
E_{1}^{ini+}	tensile initial Young's modulus in MD	3660 N/mm^2	tensile test
S_{1}^{+}	boundary tensile stress in MD	59 N/mm^2	tensile test
E_{1}^{ini-}	compressive initial Young's modulus in MD	800 N/mm^2	ring compression test
S_{1}^{-}	boundary compressive stress in MD	- 20 N/mm^2	ring compression test
E_{2}^{ini}	initial Young's modulus in ZD	13 N/mm^2	compression test

ε_{2max-}	boundary compressive strain in ZD	- 57 %	compression test
$G_{1_2}^{ini}$	initial shear moduli in the MD-ZD - plane	250 N/mm^2	shear test (glued sample)
S_{1_2}	boundary shear stress in the MD-ZD - plane	1,62 N/mm^2	shear test (glued sample)
$A_{S_{12}}$	shear hardening parameter	1,62 N/mm^2	combined compression and shear test (glued sample)
$B_{S_{12}}$	shear hardening parameter	0,39 -	combined compression and shear test (glued sample)
μ_{1_2}	Poisson's ratio in the MD-ZD - plane	-0,005	tensile test with sample thickness measurement

Tab. 1: Determined stiffness parameters

With these determined stiffness, hardening and failure parameters the approximation between theoretically computed and experimentally measured load-deformation behavior in the MD-ZD - plane is shown in the following figures.

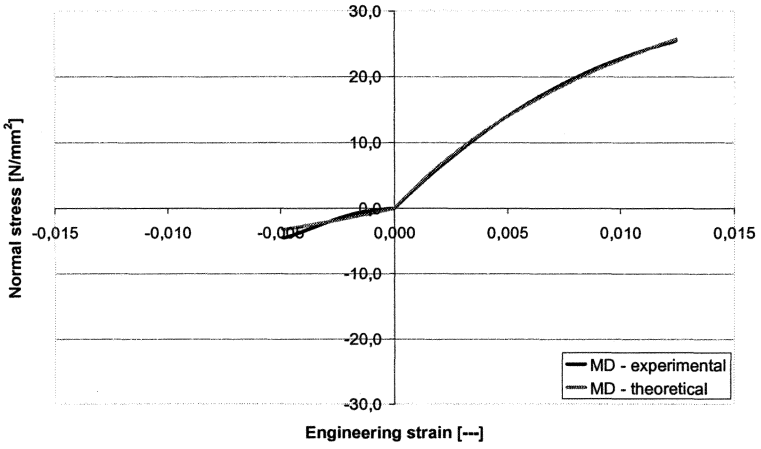

Fig. 5: Comparison theoretical computed and experimentally measured load-deformation behavior under normal load in MD

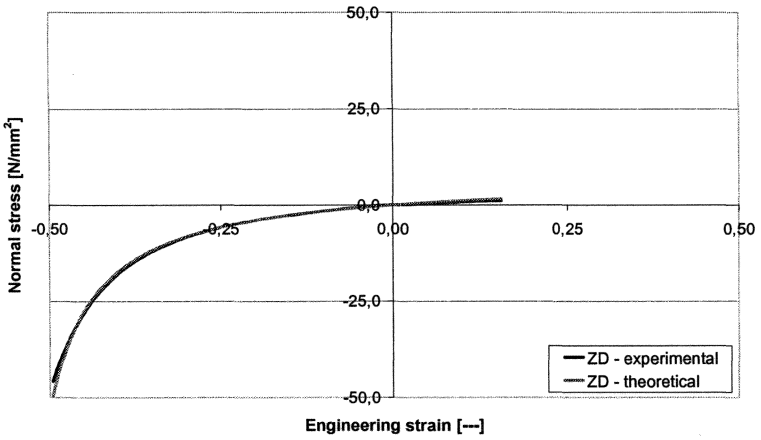

Fig. 6: Comparison theoretically computed and experimentally measured load-deformation behavior under load in ZD

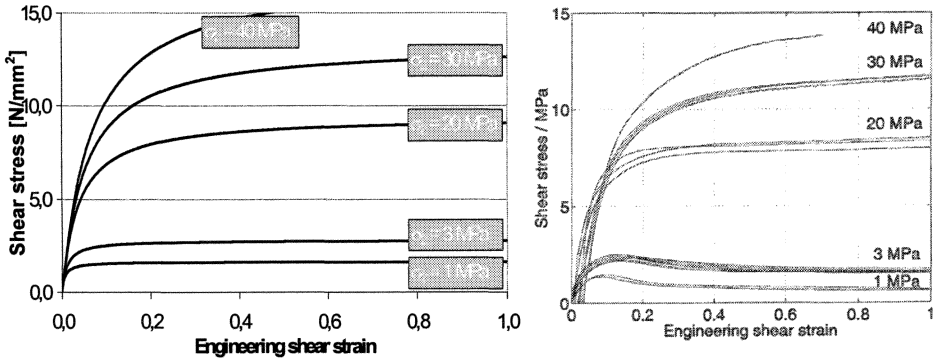

Fig. 7: Comparison theoretically computed (left figure) and by Stenberg [5] (right figure) experimentally measured load-deformation behavior under combined shear and compressive load in the MD-ZD - plane

THEORETICAL INVESTIGATION OF THE SHEAR SLITTING PROCESS

The emphasis of this analysis is the investigation of the kinetics and kinematics in the slitting zone under variation of the influence parameters of the slitting process. To perform the necessary calculations the finite-elemente-method program Marc&Mentat is used, which meets all requirements for the simulation of the slitting process such as linear and nonlinear material behavior, geometrical nonlinearities (large displacements) and nonlinear boundaries (friction contact between materials). Furthermore Marc&Mentat offers the option to add individual program enlargements in form of FORTRAN subroutines.

Basic calculation of the shear slitting of paper

Because of the kinematic analogy between longitudinal slitting and cross cutting the calculations have been carried out two-dimensionally in the MD-ZD - plane for a cross cut.

According to this a state of plane strain is assumed for all calculations. The geometrical properties of the reference model used for the basic FEM calculations are shown in fig. 8.

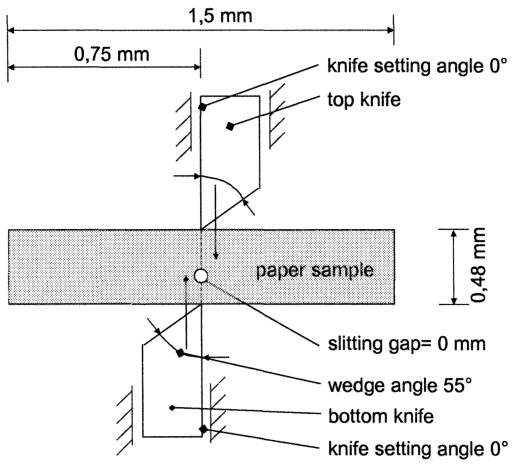

Fig 8: Geometry of the reference model

The geometric dimensions of the modeled paper sample ensure that the whole slitting area can be observed. The sample has a length of 1,5 mm, the thickness of 0,48 mm corresponds to the investigated material grade and the knives are positioned in the middle of the sample. These are modeled as rigid bodies and moved perpendicular to the sample. The displacements of the cutting tools are given as boundary conditions and are applied incrementally up to a total sample compression of 20%. The knife tip radius measures 10 µm, a value that is regarded as sharp [13] and [14].

For the FE - modeling (fig 9) square 4-nodes-elements without subnodes are used. These elements are suitable for plane strain modeling as well as for the modeling of the contact between the differing materials paper and steel. Furthermore these elements can incorporate direction dependent material properties, so that the material behavior can be modeled orthotropically. In order to discuss the occurring stresses locally a high mesh density is selected in the areas close to the knives.

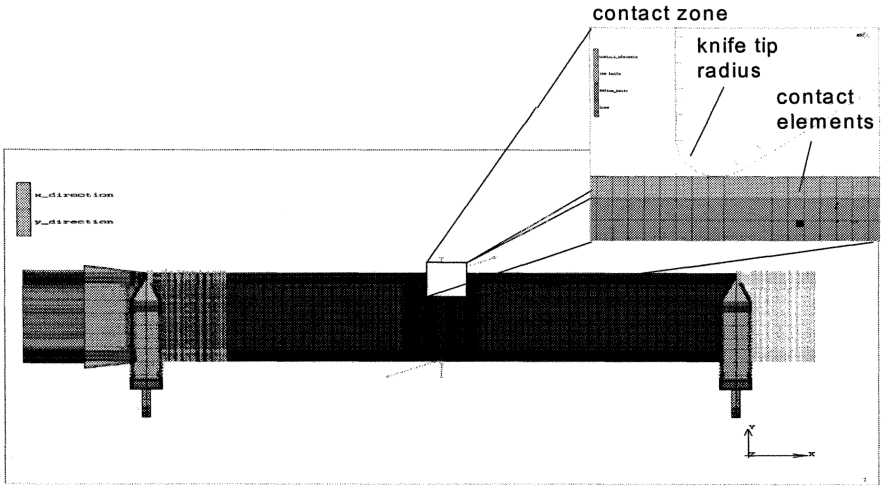

Fig. 9: FEM – reference model

For the basic understanding of the shear slitting process the described nonlinear orthotropic material law is implemented into the FEM software. The discussion of the states of stress and strain is performed locally in the area underneath the knife tip and globally in the whole slitting zone.

Results of the basic calculation of the shear slitting of paper

The aim of the basic calculations of the shear slitting process is to clarify the state of stress and strain in the slitting zone. Therefore the compression phase is investigated at a total ZD sample compression of 10 %. The calculated stresses at this state of stress and strain (fig. 10) in the slitting zone indicate, that the shear slitting process is restricted to a small area close to the knife tips. In the center of the sample all stresses drop down to zero.

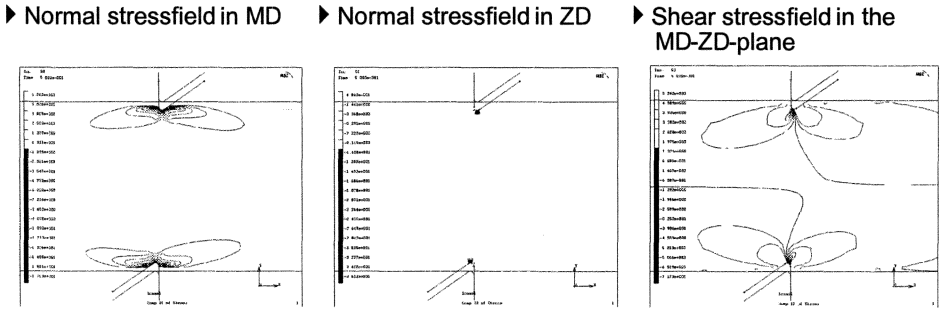

Fig. 10: Global stress fields in the slitting zone

This local stress limitation is also expressed by the stresses along the sample surface as well as by those running into the depth of the sample (fig. 11 und fig. 12).

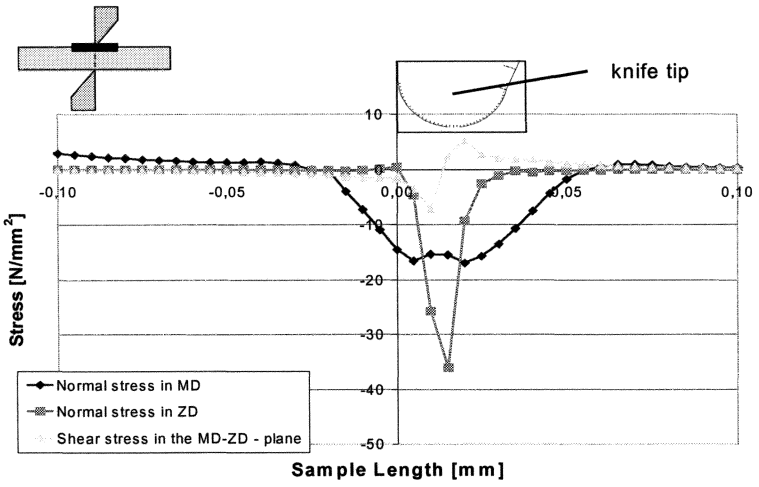

Fig. 11: Local stresses along the sample surface

Analyzing the stresses at the paper surface shows, that only in the conatct zone between knive and paper high stresses can be observed, with the highest values of the normal stresses occuring directly underneath the knife tip. The runs of the normal stresses in MD and ZD have a conical characteristic similar to the Hertz theory. The value of the shear stress rises from zero at the knife tip to its highest values at both flanks of the knive.

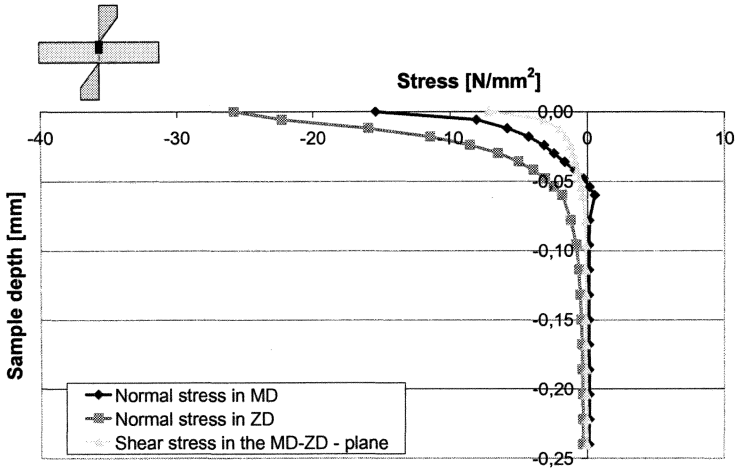

Fig. 12: Local stresses in direction to the sample middle

With regard to the material failure (right part of fig. 3) a failure parameter was implemented into the FEM software to allow an interpretation of the stresses in the slitting zone. This parameter describes the state of stress in direct comparison to the failure boundaries of the material. The higher its value, the more probable material failure is at this point. The values calculated for the failure parameter in the slitting zone are pointing to an

existence of two areas of high failure probability close to the knife flanks, running in direction of high shear stresses.

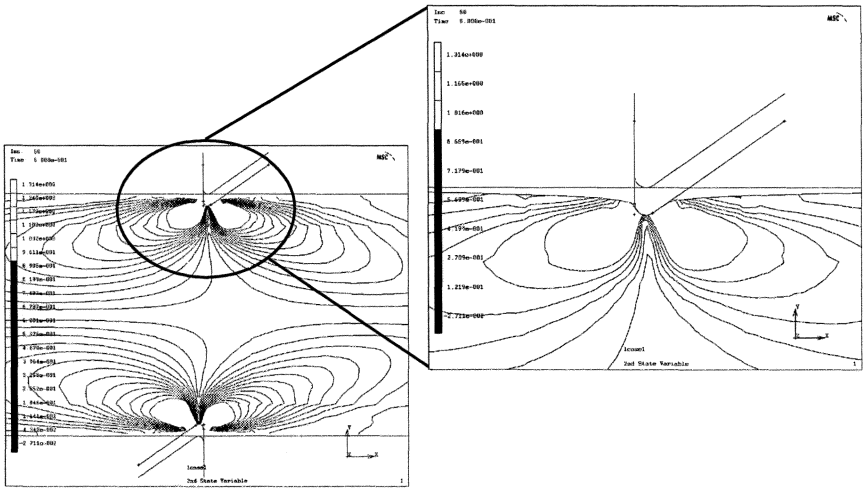

Fig. 13: Failure areas expressed by the failure parameter in the slitting zone

Application oriented calculation of the shear slitting of paper

Based on the results of the basic calculations a total ZD sample compression of 10 % is used for the variation of the individual influence parameters according to fig. 14. The chosen parameters are an extract of the most important of all possible influence parameters of the shear slitting process

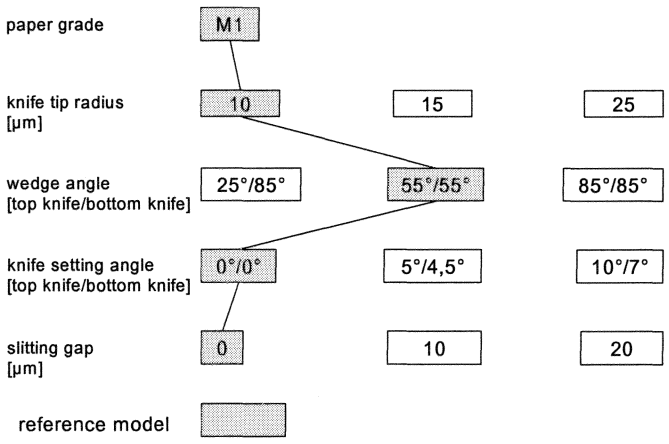

Fig. 14: Influence parameter variation

Influence of the knife tip radius on the state of stress and strain in the slitting zone

The first investigated parameter is the knife tip radius. When the knife penetrates the material, the knife tip generates the direct contact between knife and slitted material and therefore its geometry has a strong influence on the kinetics of the slitting zone. With

decreasing knife tip radius the area where the slitting forces are applied on the material gets smaller and occuring stresses rise (fig. 15).

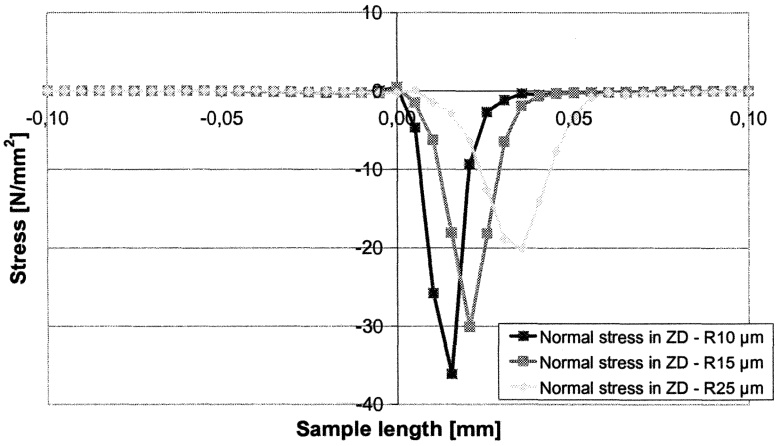

Fig. 15: Results of the knife tip radius variation: normal stresses in ZD

The results prove, that through the locally limited contact area the smallest knife tip radius generates the highets ZD stresses. For the highest investigated radius of 25 µm the stresses decrease by more than 40 %. Analog to that also the MD-ZD - shear stress decreases with higher knife tip radius (fig. 16).

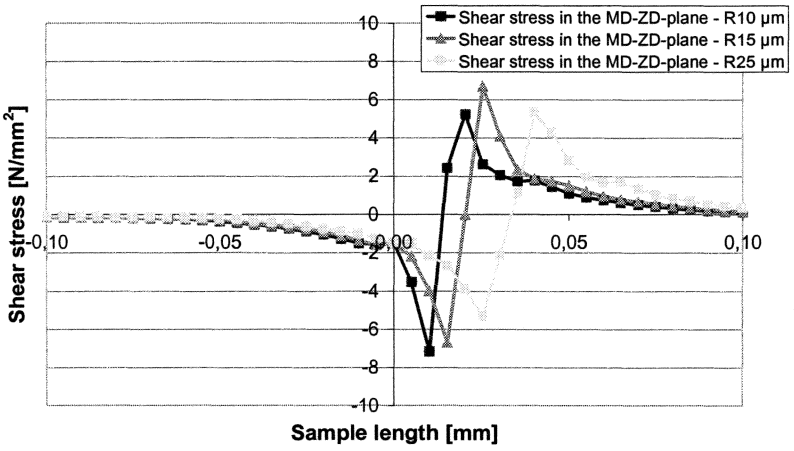

Fig. 16: Results of the knife tip radius variation: shear stresses in the MD-ZD – plane

Influence of the wedge angle on the state of stress and strain in the slitting zone

The next investigated parameter of the slitting process is the wedge angle. Again a smaller geometry in direct contact with the slitted material leads to higher stress values (fig. 17 and fig. 18)). The greater the wedge angle, the higher the deformation range of the slitting zone becomes.

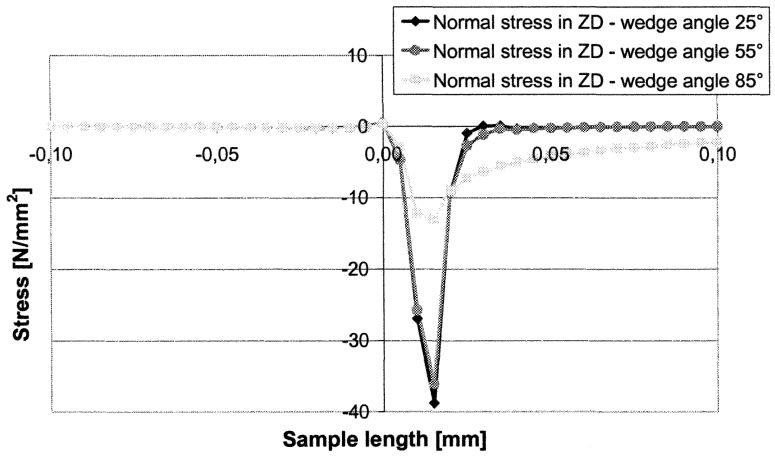

Fig. 17: Results of the wedge angle variation: normal stresses in ZD

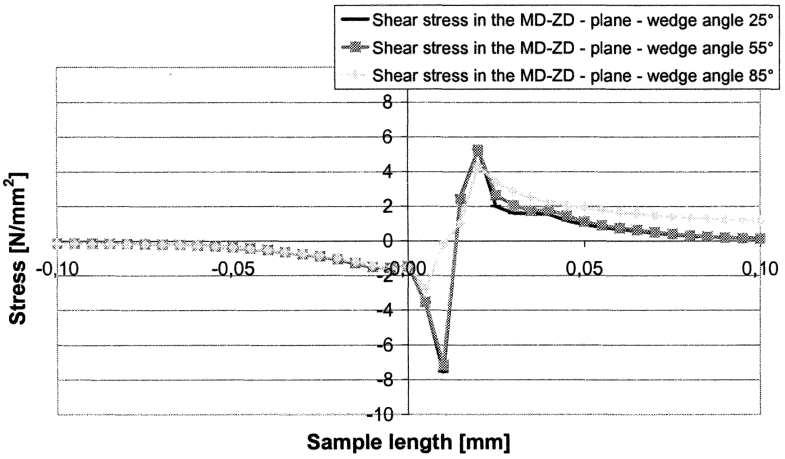

Fig. 18: Results of the wedge angle variation: shear stresses in the MD-ZD - plane

Influence of the knife setting angle on the state of stress and strain in the slitting zone

Another investigated parameter of the slitting process is the knife setting angle with the results not showing a significant influence on the kinetics of the slitting zone. Fig. 19 illustrates a summary of the calculated normal and shear stresses.

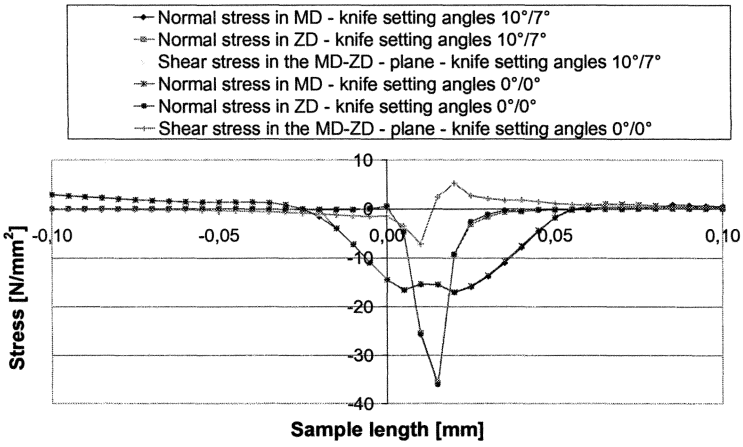

Fig. 19: Results of the knife setting angle variation: all stresses in the MD-ZD-plane

Influence of the slitting gap on the state of stress and strain in the slitting zone

Similar to the results of the knife setting angle variation the results of the slitting gap variation show no significant influence on the local state of stress close to the penetrating knife. At a gap of 20 µm the failure parameter shows a small decrease at the flanks of the knife fig 20).

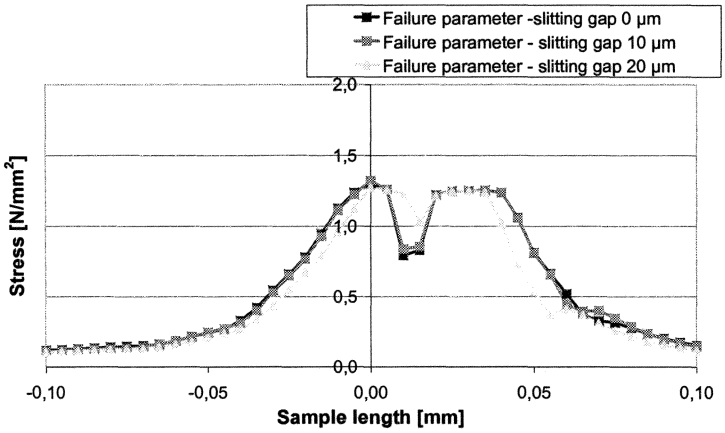

Fig. 20: Results of the slitting gap variation: failure parameter

With an increasing slitting gap the areas of slitting intiation at top and bottom knife displace from each other resulting in a poor slit quality (fig. 21).

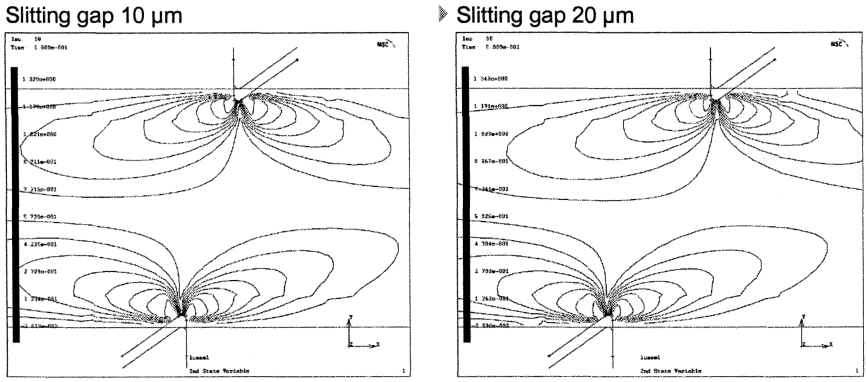

Fig. 21: Results of the slitting gap variation: failure parameter

CONCLUSION

For the optimization of the shear slitting process with regard to cut quality and blade durability the knowledge of the interdependencies between slitted material, slitting process and slitting tool is necessary.

The results of the basic investigation of the shear slitting process showed, that the knive induced stresses in the slitting zone are locally limited to a small area close to the penetrating knifes. The initiation of slitting, the transition between the compression and the slitting phase, takes place in two areas at the knive flanks, where high compressive and shear stresses occur. The variation of the slitting tool geometry showed the influences of the individual parameters on the local state of stress in the slitting zone. For the used material the smallest investigated knife tip radius and wedge angle should be used for a good slit. The variation of the slitting unit parameters showed no significant influence on the local state of stress underneath the knives. A modification of the slitting gap only changed the global state of stress in the slitting zone.

REFERENCES

1 Stroppel, Th.: *Zur Systematik der Technologie des Schneiden* Grundlagen der Landtechnik, 11. Konstrukteurheft, 2. Teil, Heft 5 (1953)

2 Feiler, M.: Ein Beitrag zur Klärung der Vorgänge beim Schneiden dünner flächiger Materialien, Dissertation 1970; Universität Stuttgart

3 Welp, E.G.; Wolf, E.: *Theoretical analysis of shear slitting of paper on the basis of a three-dimensional material law*, Proceedings of the Fifth International Conference on Web Handling, Stillwater/Oklahoma/USA (1999), ISBN 0-9654616-2-9

4 Paetow, R.: *Über das Spannungs-Verformungs-Verhalten von Papier,* Dissertation, Technische Hochschule Darmstadt 1991

5 Stenberg, N.: On the out-of-plane mechanical behavior of paper materials, Doctoral Thesis No. 51, Royal Institute of Technology, Stockholm 2002, ISSN 1104-6813

6 Ruvo, A. d.; Carlsson, L.; Fellers, C.: *The biaxial strength of paper* TAPPI, Vol. 63 (1980), Nr. 5, S. 133-136

7 Tryding, J.: A Modification of the Tsai-Wu failure criterion for the biaxial

strength of paper, Tappi Journal (1994), Heft 8, S. 132-143

8 Gunderson, D. E.; Bendtsen, L. A.; Rowlands, R. E.: *A mechanistic perspective of the biaxial strength of paperboard,* Journal of Engineering Materials and Technology, Vol. 108 (1986), S. 135-140

9 Waterhouse, J. F.: *The failure envelope of paper when subjected to combined out-of-plane stresses,* Tappi Proceedings, Paper Physics Conference (1991), S. 629 - 639

10 Xia, Q.S.; Boyce, M.C.; Parks, D.M.: Mechanics of inelastic deformation and delamination in paperboard, A constitutive model for the anisotropic elastic-plasticdeformation of paper and paperboard, International Journal of Solids and Structures 39 (2002) 4053 – 4071, ISSN 0020-7683

11 van Haag, R.: Über die Druckspannungsverteilung und Papierkompression im Walzenspalt eines Kalanders, Dissertation, Technische Hochschule Darmstadt, 1993

12 Pfeiffer, D.: *Measurement of the K2 Factor for Paper,* Tappi Journal 64 (1981), Nr. 4, S. 105-106

13 Klingelhöffer, H.: *Schneidenschärfe von Messern,* Allgemeine Papierrundschau 1, 17, (1953)

14 H. Hofer, *Stanzen von Karton und Wellpappe in Theorie und Praxis* , Papier und Kunststoffverarbeiter, Vol. 2, 1997, pp. 28 -33.